Journal of Solid State Chemistry **154,** 199–203 (2000)
doi:10.1006/jssc.2000.8836, available online at http://www.idealibrary.com on IDEAL®

Production of α-Rhombohedral Boron by Amorphous Boron Crystallization

S. O. Shalamberidze, G. I. Kalandadze, D. E. Khulelidze, and B. D. Tsurtsumia

The Institute of Stable Isotopes, 21, Kavtaradze str., Tbilisi, 380086, Georgia

Received September 9, 1999; in revised form February 10, 2000; accepted February 15, 2000

Some characteristic features of the technology of producing α-rhombohedral boron by amorphous powder crystallization were considered. Powder samples were heated in a high-temperature resistance furnace at 8°C/min to 1000°C and then the rate was reduced to 2°C/min. After the above heating rates, pyrolytic amorphous boron transforms to α-rhombohedral boron when held for 90 min at 1170°C in either argon atmosphere or vacuum. Electrolytic amorphous boron starts to crystallize at 1150°C to β-rhombohedral boron without going through the intermediate α-rhombohedral boron phase. The investigation of the influence of impurities on the crystallization of amorphous boron showed that carbon was more unfavorable than metallic impurities, preventing the formation of the α-rhombohedral boron phase. Though the powders of pyrolytic and electrolytic amorphous boron are distinguished by purity (electrolytic boron is more contaminated), the investigations performed lead to the speculation that the crystallization process is influenced by the short-range order of the atoms of the initial powders rather than by the impurity content. © 2000 Academic Press

Key Words: **amorphous boron; crystallization; structure; α-rhombohedral boron; β-rhombohedral boron.**

INTRODUCTION

Of the crystalline modifications of boron, α-rhombohedral, tetragonal, and β-rhombohedral, the β-rhombohedral modification of boron has been the most studied. This is due to the fact that the α-rhombohedral as well as the tetragonal modifications of boron are metastable and irreversibly transform to the β-rhombohedral modification when subjected to thermal treatment. Earlier investigations (1–4) of the α-rhombohedral boron properties report some of the characteristic features of this modification of boron. Therefore, the improvement of the technological methods of producing high-quality α-rhombohedral boron with a view to investigating its properties is the goal of the present study.

We believe that amorphous boron crystallization is the most suitable method for high-quality α-rhombohedral boron sample production. Other studies (5–14) devoted to the investigation of the technological parameters of amorphous boron crystallization assert that amorphous boron crystallization is similar to that of glassy materials; i.e., the presence of nucleation sites is more important than specific temperature conditions. For this reason the presence of impurities in amorphous boron is of a great significance. Boron oxide (B_2O_3) and boron suboxide (B_6O) are supposed to be favorable impurities in α-rhombohedral boron production (6, 7, 11). Other references (9, 11, 12) report that even low concentrations of metallic impurities impede the formation of the α-rhombohedral modification of boron. Amberger *et al.* (5) assert that the formation of a variety of the crystalline modifications of boron depends more on purity of the initial material rather than on the temperature.

Bairamashvili (13) gives the results of the crystallization study of amorphous boron powders produced by diborane pyrolysis and potassium tetrafluoroborate electrolysis. A high-temperature X-ray investigation showed that pyrolytic amorphous boron was crystallized as α-rhombohedral modification at 1270°C. As the temperature rose, the sample transformed to the β-rhombohedral modification. Under identical experiments, electrolytic amorphous boron started to be transited to the β-rhombohedral modification at 1200°C. Based on the atom radial distribution investigations of the amorphous boron powders, the authors concluded that the powders of pyrolytic and electrolytic amorphous boron are distinguished by the nature of their short-range order and so the formation of different crystalline modifications of boron depend on substructure of the initial amorphous powders.

The results on the study of the effect of some technological parameters on amorphous boron crystallization process are presented in this work as an addition to earlier data.

EXPERIMENTAL

Two types of powders were used for the investigation of the amorphous boron crystallization process: pyrolytic amorphous boron produced by diborane cracking and

0022-4596/00 $35.00
Copyright © 2000 by Academic Press
All rights of reproduction in any form reserved.

TABLE 1
The Impurity Content (in wt%) of Electrolytic Amorphous Boron

	Mn	Mg	Si	Fe	Ni	Al	Ca	Cu	C
Lot 1	0.014	0.08	0.04	0.4	0.3	0.01	0.001	0.1	0.6
Lot 2	0.003	0.045	0.02	0.1	0.08	0.01	0.001	0.05	0.3

electrolytic amorphous boron produced by the electrolysis of potassium tetrafluoroborate.

Pyrolytic amorphous boron used in these experiments had the purity of 99.7 wt%; the content of the metallic impurities did not exceed 0.2 wt% and that of carbon −0.1 wt%.

Electrolytic amorphous boron used in these experiments was manufactured at the Institute of Stable Isotopes (Tbilisi). Its metallic impurities did not exceed 0.6 wt% and that of the carbon −0.6 wt% (Table 1). Lot 1 electrolytic amorphous boron powder was a common serial product and lot 2 powder was made under special conditions and subjected to careful chemical purifying.

The amorphous powders of boron were crystallized in a high-temperature resistance heated furnace under argon at atmospheric pressure and 10^2 Pa vacuum. The samples were prepared in the form of pellets of 1 g/cm^3 density by the cold pressing method. The heating rate was 8°C/min up to 1000°C. Subsequently, the heating rate was reduced to 2°C/min. Under such conditions the samples were heated to the temperature of crystallization and held at this temperature for some time. After cooling, the samples were removed from the furnace for structural examination with an X-ray diffractometer using Fe$K\alpha$ radiation.

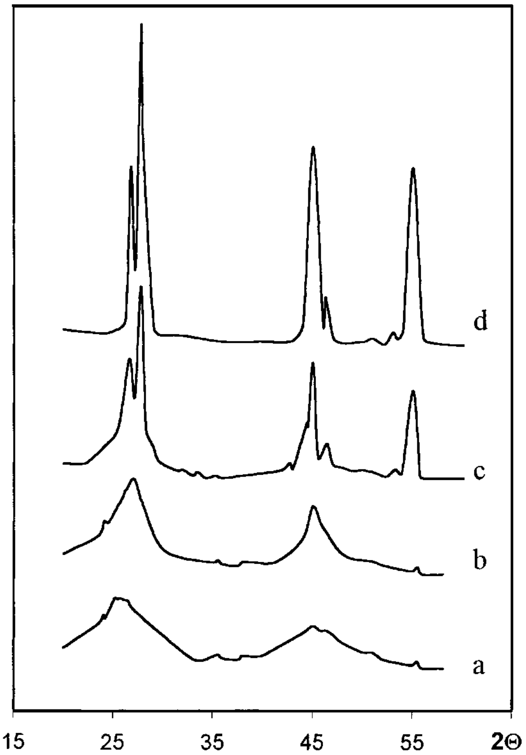

FIG. 1. X-ray diffraction patterns after crystallization (hold time, 90 min) for the samples of pyrolytic amorphous boron: (a) $T = 1140$°C, (b) $T = 1150$°C, (c) $T = 1160$°C, (d) $T = 1170$°C.

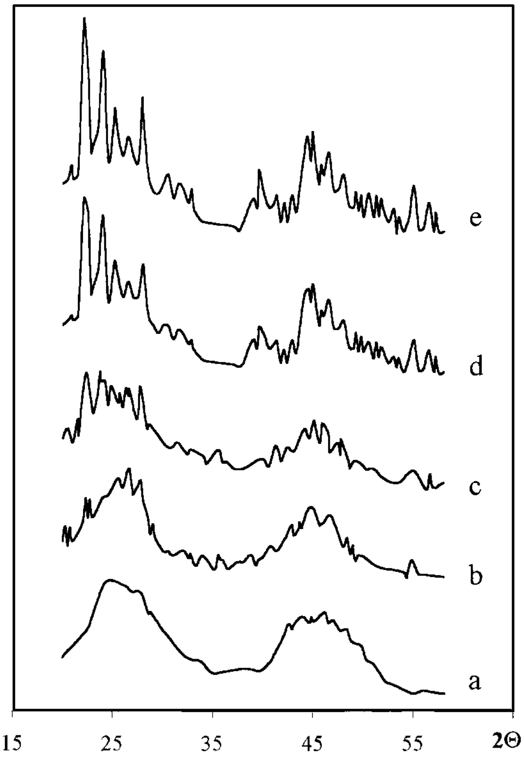

FIG. 2. X-ray diffraction patterns after crystallization (hold time, 90 min) for the samples of electrolytic amorphous boron. (a) $T = 1130$°C, (b) $T = 1140$°C, (c) $T = 1150$°C, (d) $T = 1160$°C, (e) $T = 1170$°C.

RESULTS AND DISCUSSION

In the course of the experiments carried out with the samples of pyrolytic amorphous boron, the optimum conditions for amorphous boron crystallization were determined to be 1170°C with a hold time of 90 min. The X-ray patterns on Fig. 1 show that the samples of pyrolytic amorphous boron retain the amorphous structure up to 1140°C. At 1150°C, the amorphous halos narrow and their peak intensities rise. A further increase in the crystallization temperature to 1160°C leads to the occurrence of the peaks characteristic of α-rhombohedral boron, and at 1170°C the sample has the complete structure of α-rhombohedral boron.

The X-ray diffraction patterns of the samples made by electrolytic boron powder crystallization are shown in

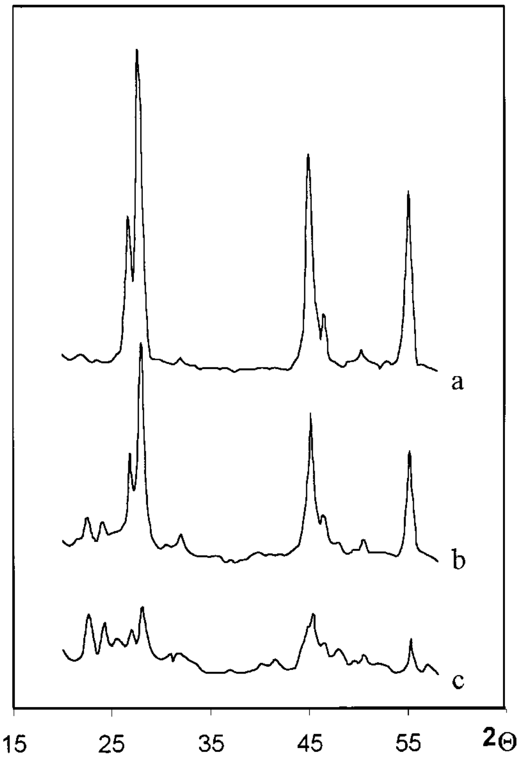

FIG. 3. X-ray diffraction patterns after crystallization ($T = 1170°C$; hold time, 90 min) for the samples of pyrolytic amorphous boron: (a) pyrolytic amorphous boron (the control), (b) pyrolytic amorphous boron + 0.5 wt% Fe + 0.5 wt% Ni, (c) pyrolytic amorphous boron + 1.5 wt% Fe + 1.5 wt% Ni.

Fig. 2. Amorphous boron starts to be crystallized at 1140°C—with peaks characteristic of β-rhombohedral boron observed above the amorphous halo. As the temperature rises, the number and the intensities of the peaks increase, and at 1170°C the structure of β-rhombohedral boron is observed, although not quite well formed. The X-ray diffraction patterns of electrolytic amorphous boron samples of both lots are almost identical.

The distinction in the crystallization processes of the amorphous powders of pyrolytic and electrolytic boron can be attributed to the differences in the technological methods of the initial powder preparation as well as in the characteristic features related to them. First of all, the difference in the purity of pyrolytic and electrolytic amorphous boron powders attracts attention.

Some experiments were performed to find out the effect of different impurities on the amorphous boron crystallization. The different concentrations of iron, nickel, and carbon impurities, which are the major impurities of electrolytic amorphous boron, were artificially introduced in pyrolytic amorphous boron. The crystallization was carried out under the above described conditions. Control samples of pure pyrolytic boron always were beside the samples under investigation.

When 0.5 wt% iron and 0.5 wt% nickel impurities are artificially introduced in pyrolytic boron, α-rhombohedral boron is still formed upon crystallization. The X-ray diffraction patterns (Fig. 3) show that the intensity of the α-rhombohedral boron typical peaks are decreasing to 60% of the pure pyrolytic boron control samples, and also the peaks typical of β-rhombohedral boron appear. When 1.5 wt% iron and 1.5 wt% nickel are introduced, the diffraction peaks of α-rhombohedral boron disappear almost entirely, while the number and the intensity of the diffraction peaks of β-rhombohedral boron increases.

The introduction of 0.2 and 0.5 wt% carbon impurity in pyrolytic boron negligibly affected the result of the crystallization process (Fig. 4). A 1 wt% carbon impurity however noticeably affects the crystallization process: the diffraction peak intensities of α-rhombohedral boron decrease to 20% of control samples. The introduction of 1.2 wt% carbon impurity leads to a total disappearance of the α-rhombohedral boron structure. Upon introducing 4 wt% boron carbide, B_4C, in pyrolytic amorphous boron the diffraction peaks of α-rhombohedral boron have 75% less intensity than the control.

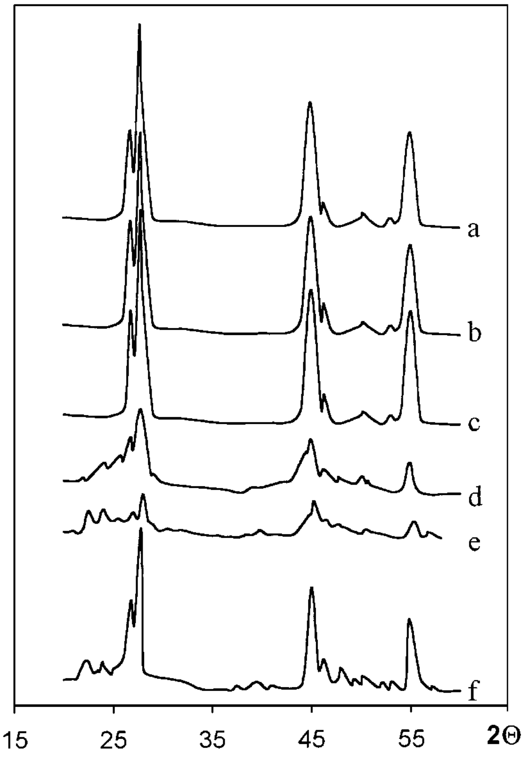

FIG. 4. X-ray diffraction patterns after crystallization ($T = 1170°C$, hold time, 90 min) for the samples of pyrolytic amorphous boron: (a) pyrolytic amorphous boron (the control), (b) pyrolytic amorphous boron + 0.2 wt% C, (c) pyrolytic amorphous boron + 0.5 wt% C, (d) pyrolytic amorphous boron + 1 wt% C, (e) pyrolytic amorphous boron + 1.2 wt% C, (f) pyrolytic amorphous boron + 4 wt% B_4C.

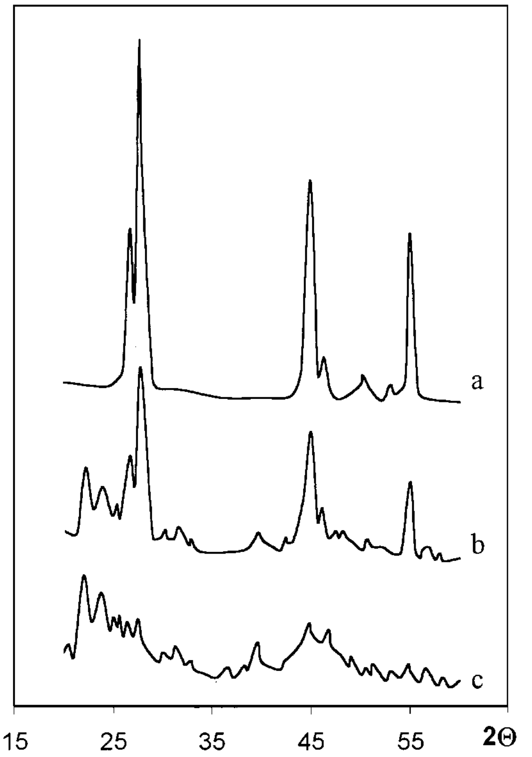

FIG. 5. X-ray diffraction patterns after crystallization ($T = 1170°C$; hold time, 90 min) for the samples of amorphous boron: (a) pyrolytic amorphous boron (the control), (b) 80 wt% pyrolytic amorphous boron + 20 wt% electrolytic amorphous boron, (c) 50 wt% pyrolytic amorphous boron + 50 wt% electrolytic amorphous boron.

The dilution of the impurities of electrolytic amorphous boron by mixing with pyrolytic boron does not result in a well formed structure of α-rhombohedral boron (Fig. 5). Upon adding 50 wt% of electrolytic amorphous boron to pyrolytic amorphous boron, the crystallized samples have the β-rhombohedral boron structure. Even the adding 20 wt% of electrolytic boron to pyrolytic boron considerably reduces the intensities of the α-rhombohedral boron diffraction peaks (50% of the control) and causes of the diffraction peaks typical of β-rhombohedral boron to appear.

Electrolytic amorphous boron fails to be transformed to crystalline α-rhombohedral boron when boric acid, H_3BO_3, is introduced as a nucleation agent (Fig. 6). Even crystals of α-rhombohedral boron do not become nucleation sites when introduced in electrolytic amorphous boron. The X-ray diffraction patterns taken after crystallizing the samples which initially contained 80 wt% electrolytic amorphous boron and 20 wt% α-rhombohedral boron show the peaks of β-rhombohedral boron along with the α-rhombohedral boron peaks (Fig. 7). The intensities of the α-rhombohedral boron peaks are only 37% of the intensity of the control peaks. The intensities of the X-ray diffraction peaks rise to 70% when the content of the α-rhombohedral boron in the sample is 50 wt%. Despite the presence of α-rhombohedral boron nucleation sites, only a small part of electrolytic amorphous boron (approximately 20% of the electrolytic boron content in the samples) is crystallized as α-rhombohedral boron.

The above experiments demonstrated some characteristic features of pyrolytic and electrolytic amorphous boron crystallization. The introduction of metallic and carbon impurities in pyrolytic amorphous boron deteriorates the crystalline structure of α-rhombohedral boron. Carbon is a more unfavorable impurity than the metallic ones. It should also be noted that the disappearance of the α-rhombohedral boron structure in the samples from pyrolytic boron is observed when the impurity concentrations substantially exceed the typical impurity contents of electrolytic amorphous boron. Even more pure electrolytic boron (Lot 2), not greatly differing from pyrolytic amorphous boron by impurity content, cannot be crystallized as α-rhombohedral boron. A decrease in the impurity concentrations of electrolytic boron by dilution with pyrolytic boron does not result in crystallization as α-rhombohedral boron either. A careful examination of the X-ray diffraction patterns indicates that in the case of the

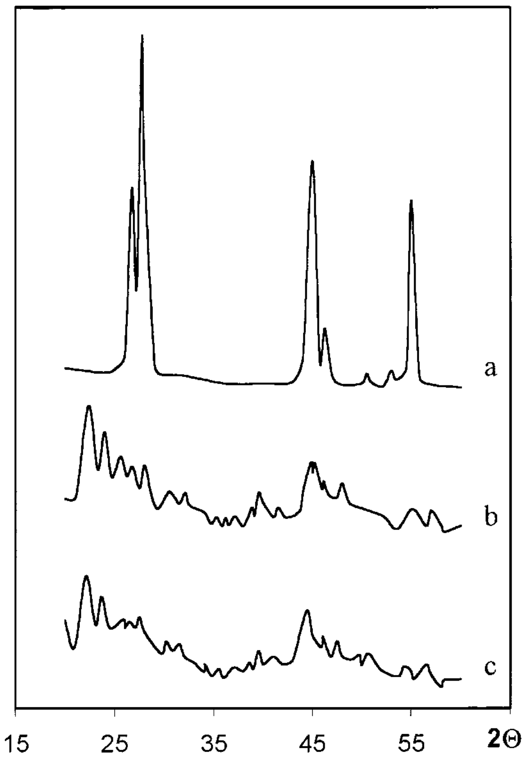

FIG. 6. X-ray diffraction patterns after crystallization ($T = 1170°C$; hold time, 90 min) for the samples of amorphous boron: (a) pyrolytic amorphous boron (the control), (b) electrolytic amorphous boron + 4 wt% H_3BO_3, (c) electrolytic amorphous boron + 7 wt% H_3BO_3.

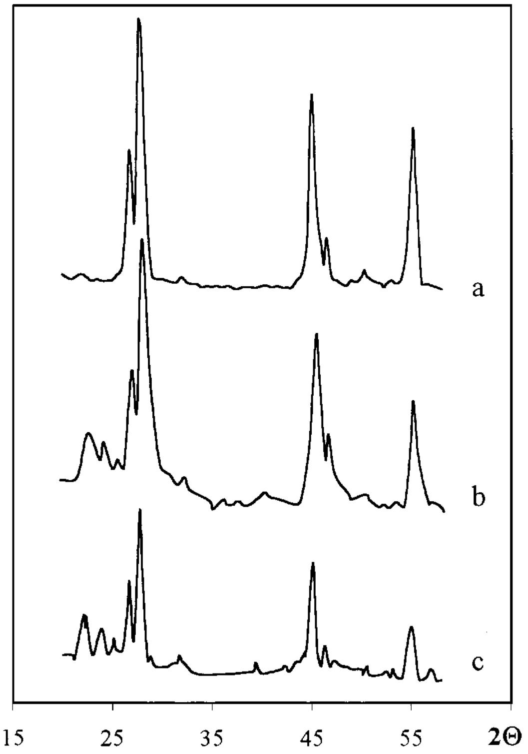

FIG. 7. X-ray diffraction patterns after crystallization ($T = 1170°C$; hold time, 90 min) for the samples of amorphous boron: (a) Pyrolytic amorphous boron (the control), (b) 50 wt% electrolytic amorphous boron + 50 wt% α-rhombohedral boron, (c) 80 wt% electrolytic amorphous boron + 20 wt% α-rhombohedral boron.

pyrolytic boron samples with artificial impurities, the deterioration of the α-rhombohedral boron structure occurs rather than the formation of the β-rhombohedral boron structure. In all samples containing electrolytic amorphous boron, the formation of the β-rhombohedral boron phase is observed.

It would be fair to note that the artificial introduction of impurities in pyrolytic amorphous boron does not exactly simulate electrolytic amorphous boron. Metallic impurities as well as carbon can be present in different forms in electrolytic amorphous boron. The major source of these impurities is the Monel metal cathode, salts (KBF_4, KCl), and a graphite anode crucible. We believe that various impurities are present in electrolytic amorphous boron as atomic inclusions and solid solutions of various borides, carbides, and fluorides. We speculate that these ultimately affect the microstructure and the short-range order of the atom arrangement in electrolytic amorphous boron.

The preliminary results on the investigations of the short-range order of the atom arrangement in pyrolytic and electrolytic amorphous boron indicate some structural features. The complete results of these investigations will be published later.

CONCLUSION

This investigation demonstrates that the crystallization of amorphous powders of pyrolytic boron and that of electrolytic boron start at the same temperature. Pyrolytic boron is crystallized as α-rhombohedral boron, while electrolytic boron crystallizes as the β-rhombohedral modification without going through the intermediate stage of α-rhombohedral boron. These distinctions in the crystallization processes are indirectly brought about by the different impurity contents of the initial amorphous boron. The specific character of the technological process of electrolysis leads to amorphous boron contamination with metallic and carbon impurities, which are implanted in the boron lattice as various borides, carbides, and fluorides causing a change in the microstructure of electrolytic amorphous boron. The short-range order of the atom arrangement in the microstructure of different-origin amorphous boron is the factor that affects the crystallization processes.

REFERENCES

1. I. A. Bairamashvili, J. Sh. Jobava, and G. I. Kalandadze, *Izv. Akad. Nauk USSR Neorg. Mater.* **19**(2), 214 (1983).
2. D. Tsiskarishvili, G. Tsagareishvili, and J. Omiadze, *et al.*, *J. Less-Common Metals* **117,** 143 (1986).
3. H. Werheit *et al.*, *in* "Boron-Rich Solids" (D. Emin, Ed.), AIP Conference Proceedings 231, p. 350. New York, 1991.
4. K. Shirai and H. Katayama-Yoshida, *Physica B* **263–264**(1), 791 (1999).
5. E. Amberger, W. Dietze, J. Jaumann, and P. Runow, *Phys. Solid State A.* (*Germany*) **2**(2), 59 (1970).
6. Y. A. Ugai, N. E. Solovév, E. M. Averbakh, and A. M. Parfenov, *in* "Boron, Preparation, Structure and Properties" (F. H. Tavadze, Ed.), p. 18. Nauka, Moscow, 1974.
7. J. A. Ugai and N. E. Soloviev, *in* "Boron and Refractory Borides" (Matkovich, Ed.), pp. 227–240. Springer, Berlin, 1977.
8. J. S. Gillespie, *J. Am. Chem. Soc.* **88**(11), 2423 (1966).
9. R. M. Pirtskalaishvili and I. A. Bairamashvili *et al.*, *in* "Boron, Preparation, Structure and Properties" (F. H. Tavadze, Ed.), p. 23. Nauka, Moscow, 1974.
10. N. E. Soloviev, V. S. Makarov, and Ya. A. Ugai, *J. Less-Common Metals* **117,** 21 (1986).
11. E. M. Averbakh, N. E. Solovév, and Ya. A. Ugai, Authors Certificate 331661. USSR, 1973.
12. V. P. Genzenko, N. E. Solovév, and Ya. A. Ugai, Authors Certificate 458510. USSR, 1975.
13. I. A. Bairamashvili *et al.*, *Neorg. Mater.* (*USSR*) **20**(3), 409 (1984).
14. T. G. Jandieri, G. I. Kalandadze, and P. J. Kervalishvili, *Neorg. Mater.* (*USSR*) **24**(12), 1982 (1988).